System-Size Effects and Scaling Laws in Nanoscale Droplet Wetting

Naveen Kumar Subramanian[1] Nikos Savva[1,2] Vangelis Harmandaris[1]

[1]The Cyprus Institute, Nicosia, Cyprus [2]University of Cyprus, Nicosia, Cyprus

n.k.subramanian@cyi.ac.cy

Abstract

Wetting dynamics at the nanoscale provide an important link between molecular interactions and continuum-scale behaviour. We use molecular dynamics (MD) simulations to investigate the effects of system size and surface wettability on water droplets spreading over silica substrates. Droplets with initial radii of $R_0 = 5$, 10, and 20 nm are studied across different equilibrium contact angles. Post-processed density contours are used to track the evolving droplet geometry, contact radius, and relaxation toward equilibrium. The simulations recover an early-time neck-growth regime consistent with $t^{1/2}$ scaling, followed by viscous-dominated spreading approaching the $t^{1/10}$ scaling for sufficiently large systems. Normalization using characteristic viscous timescales reveals the underlying size dependence and provides a connection between atomistic wetting dynamics and continuum scaling laws.

1. Water droplet on silica: molecular dynamics

Spherical water droplets placed in contact with a silica surface (equilibrium contact angle $\theta_e \approx 86°$). Three initial radii, $R_0 = 5$, 10, and 20 nm, are used to examine system size effects.

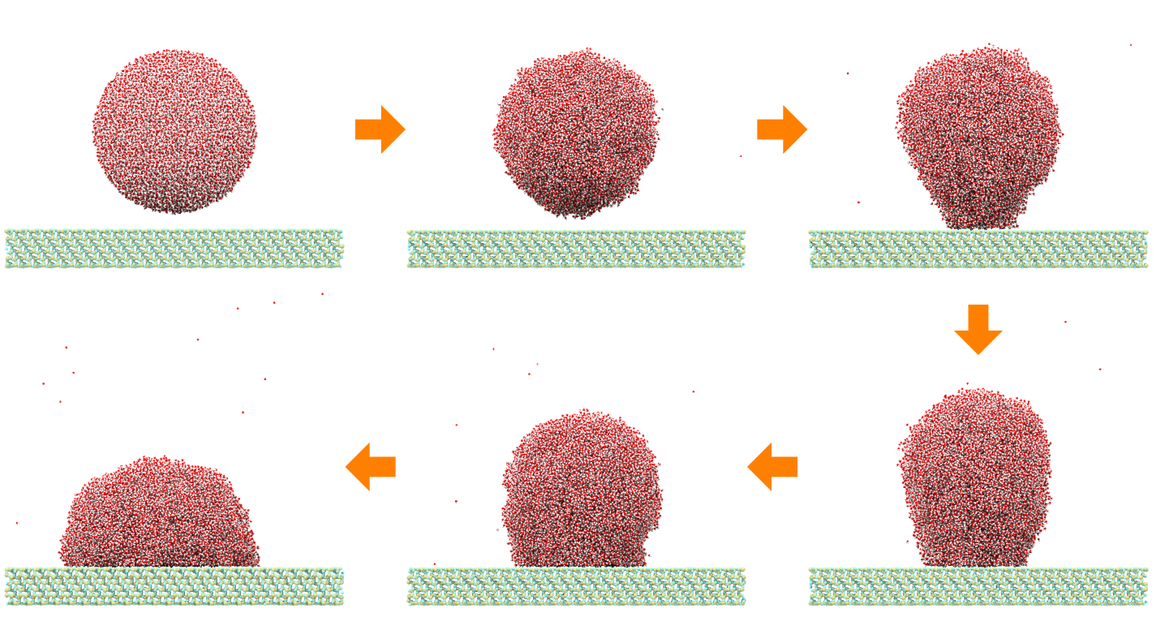

Snapshots of a droplet with $R_0 = 20\,\mathrm{nm}$ evolving towards equilibrium.

Parameter	$R_0 = 5$ nm	$R_0 = 10$ nm	$R_0 = 20$ nm
Water molecules	2,022	18568	130,408
Silica atoms	20,829	86,416	341,264
Total atoms	26,895	142,120	732,488
Simulation duration	10 ns	20 ns	30 ns
Ensemble		NVT	
Temperature		300 K	
Electrostatics		Particle mesh Ewald (PME)	

2.Effect of Bin size on interface extraction

The influence of spatial resolution is examined using different bin sizes Δx. ForΔx, the interface is identified using the same half-bulk-density criterion. Smaller Δx gives more density fluctuations , while bit larger bin sizes gives smooth profile and is show in figure 1.

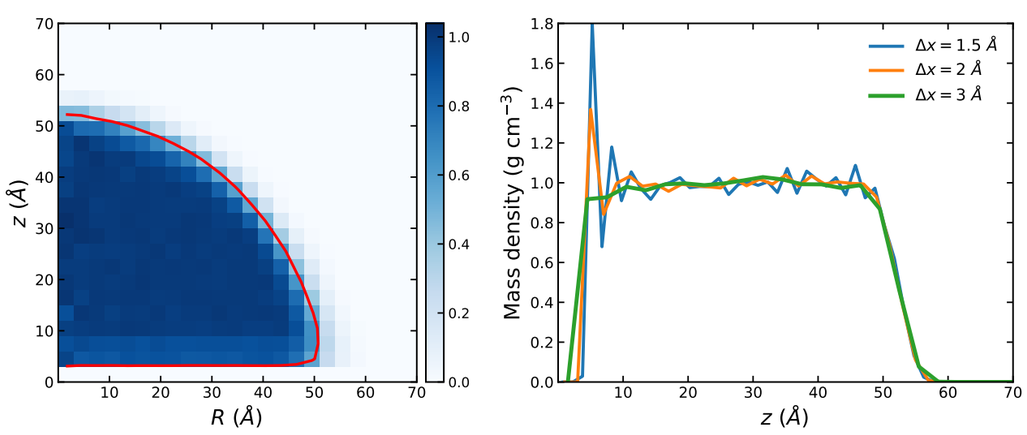

Figure 1. **Left:** Equilibrium water mass-density field obtained with $\Delta x = 3$; the red contour denotes the interface at $\rho^* \approx 0.5\ \mathrm{g\,cm^{-3}}$. **Right:** Mass-density profiles obtained using different spatial bin sizes

3. Ensemble-averaged interfacial profile extraction

To reduce molecular-scale fluctuations, water oxygen coordinates from ten independent MD simulations are transformed into cylindrical coordinates (R, z) and binned to construct the ensemble-averaged Number-density $\rho(R, z)$.
The resulting contours provide a smooth representation of the evolving droplet interface and are approximate to curvature to determine the contact radius $R(t)$, droplet height $h(t)$, and dynamic contact angle $\theta(t)$.

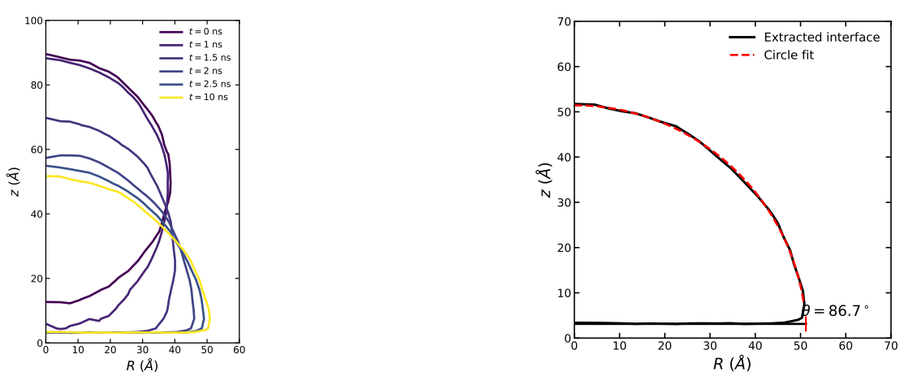

Figure 2. **Left:** Evolution of the ensemble-averaged interface extracted from the water density field at different times. **Right:** Circle fit to the equilibrium interface used to calculate equilibrium contact angle.

4. Silica hydroxylation controls wettability

The wettability of the silica surface is varied by changing the surface Si–OH concentration. Increasing the hydroxyl concentration strengthens the interaction of water with the surface, resulting in greater spreading and a lower equilibrium contact angle.
As shown in Fig. 3, the equilibrium contact angle decreases systematically with increasing Si–OH concentration.

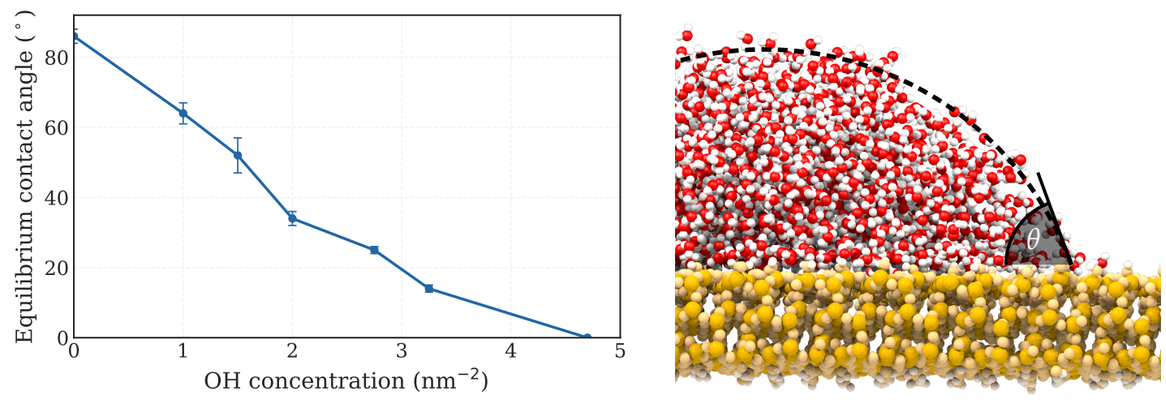

Figure 3. **Left:** Equilibrium contact angle as a function of surface Si–OH concentration, showing increased wettability with increasing hydroxylation. **Right:** Equilibrated water droplet on the silica surface, illustrating a surface concentration of approximately $1.2\ \mathrm{nm^{-2}}$ gives $\theta_e \approx 65°$.

5. Inertial and viscous scaling across wettabilities

For each equilibrium contact angle, we compare droplets with $R_0 = 5$, 10, and 20 nm using the normalized contact radius r/R_0. The characteristic inertial and viscous times are

$$\tau_i = \sqrt{\frac{\rho R_0^3}{\gamma}}, \qquad \tau_v = \frac{\mu R_0}{\gamma},$$

where ρ is the liquid density, μ its dynamic viscosity, and γ the liquid–vapour surface tension. The left column plots r/R_0 against t/τ_i with a $t^{1/2}$ reference slope. The right column plots r/R_0 against t/τ_v with a $t^{1/10}$ reference slope. We use these plots to compare the size dependence and identify the time ranges where each scaling behaviour is observed.

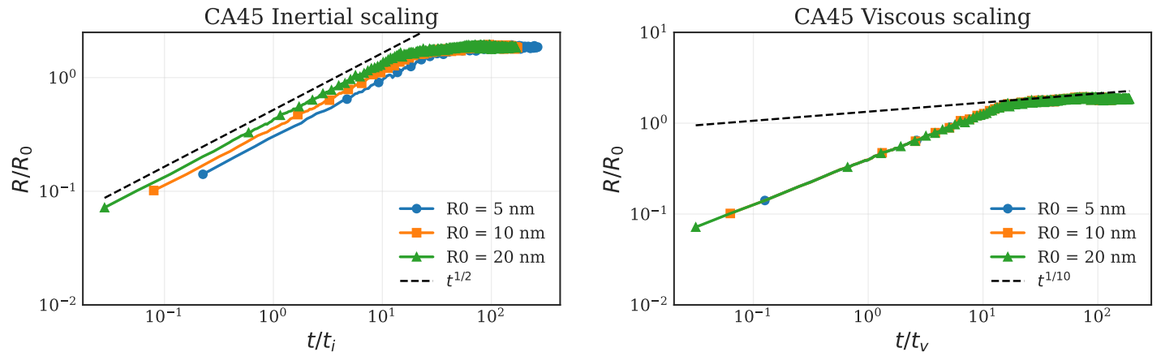

Figure 4. Size-dependent spreading for CA45 Left: inertial-time scaling. Right: viscous-time scaling. Each plot compares $R_0 = 5$, 10, and 20 nm. Similar studies has been done for different Contact angles and shows same pattern

Conclusion and Further Study

Molecular dynamics simulations were used to study the spreading of nanoscale water droplets on silica surfaces.
Droplets with different initial sizes and surface wettabilities were compared using the evolution of the contact radius and contact angle.
Future work will extend the current water–silica study to other liquid–surface systems. In particular, polymer systems such as polyethylene (PE) on silica will be investigated.
The molecular-scale results will also support the development of continuum models.

References

1. L. H. Tanner, "The spreading of silicone oil drops on horizontal surfaces," *J. Phys. D: Appl. Phys.* **12**, 1473–1484 (1979). doi:10.1088/0022-3727/12/9/009.
2. P.-G. de Gennes, "Wetting: statics and dynamics," *Rev. Mod. Phys.* **57**, 827–863 (1985). doi:10.1103/RevModPhys.57.827.
3. D. Bonn *et al.*, "Wetting and spreading," *Rev. Mod. Phys.* **81**, 739–805 (2009). doi:10.1103/RevModPhys.81.739.
4. N. Tretyakov *et al.*, "Parameter passing between molecular dynamics and continuum models for droplets on solid substrates: The static case," *J. Chem. Phys.* **138**, 064905 (2013). doi:10.1063/1.4790581.

Acknowledgements

THE CYPRUS INSTITUTE
RESEARCH·TECHNOLOGY·INNOVATION

Co-funded by the European Union

This work is partly funded by the European Union's Horizon 2020 Research and Innovation Programme under the Marie Skłodowska-Curie COFUND scheme, grant agreement No. 101034267.